

Research Article

Synthesis and Characterization of Single-Crystalline SnO₂ Nanowires

Dezhou Wei, Yanbai Shen, Mingyang Li, Wengang Liu, Shuling Gao, Lijun Jia, Cong Han, and Baoyu Cui

College of Resources and Civil Engineering, Northeastern University, Shenyang 110819, China

Correspondence should be addressed to Yanbai Shen; yanbai.shen@gmail.com

Received 7 May 2013; Accepted 22 September 2013

Academic Editor: Xinqing Chen

Copyright © 2013 Dezhou Wei et al. This is an open access article distributed under the Creative Commons Attribution License, which permits unrestricted use, distribution, and reproduction in any medium, provided the original work is properly cited.

Tin oxide (SnO₂) nanowires were synthesized on oxidized silicon substrates by thermal evaporation of tin grains at 900°C in Ar flow at ambient pressure. Structural characterization using X-ray diffraction and transmission electron microscopy shows that SnO₂ nanowires have a single crystal tetragonal structure. Scanning electron microscopy observation demonstrates that SnO₂ nanowires are 30–200 nm in diameter and several tens of micrometers in length. The surface vibration mode resulting from the nanosize effect at 565.1 cm⁻¹ was found from the Fourier transform infrared spectrum. The formation of SnO₂ nanowires follows a vapour-solid (VS) growth mechanism. The gas sensing measurements indicate that SnO₂ nanowire gas sensor obtains peak sensitivity at a low operating temperature of 150°C and shows reversible response to H₂ gas (100–1000 ppm) at an operating temperature of RT–300°C.

1. Introduction

In recent years, much more attention has been focused on the research field of quasi-one-dimensional nanostructural materials due to their importance for understanding the fundamental properties of low dimensionality and the wide range of their potential applications in nanodevices [1, 2]. SnO₂, as an n-type wide band gap semiconductor material ($E_g = 3.6$ eV at 300 K), is a key functional material that has been used extensively for transparent conductors [3, 4], gas sensors [5, 6], transistors [7], solar cells [8], and optoelectronic devices [9, 10]. So far, considerable efforts have been devoted to the research on the synthesis and characterization of SnO₂ nanomaterials such as nanowires [11, 12], nanotubes [13], nanorods [14], and nanobelts [15, 16] by using various synthetic methods. Among these methods, thermal evaporation is widely used because of its simple operation, low cost in preparation, and large-scale production.

SnO₂ nanomaterials are very promising for gas sensors due to their advantageous characteristics of large surface-to-volume ratio and great surface activity. Gas sensors based on SnO₂ nanomaterials have shown higher sensitivity, faster response, and enhanced capability to detect low concentration gases compared with the corresponding thin film

materials [16, 17]. However, most of them are effective at high temperature above 200°C, which results in high power consumption and complexities in integration. Therefore, there is a need to develop SnO₂ nanomaterials for gas sensors that have good performance at a low temperature. In addition, much more efforts have been devoted to study the CO, NO₂, or ethanol gas sensing properties of SnO₂ nanomaterials [15–20], and only a few reports were related to H₂ gas sensing properties [21–23]. Deshpande et al. [21] reported that Pt-catalyst SnO₂ nanowires could detect 500 ppm H₂ gas with response time as low as 10 sec at RT. Wang et al. [22] reported that the response of SnO₂ nanowires to 500 ppm H₂ gas could be repeated without observing major changes in the signal at RT. Kolmakov et al. [23] reported that individual Pd-functionalized SnO₂ nanowires and nanobelts exhibited a dramatic improvement in the sensitivity toward oxygen and hydrogen at 200 and 270°C. However, in their works, the responses of SnO₂ nanowires were investigated only under the fixed temperature and H₂ concentration.

In this study, single-crystalline SnO₂ nanowires were synthesized by thermal evaporation of tin grains at 900°C in an Ar flow at ambient pressure. Structural characterization of the obtained SnO₂ nanowires was investigated by using X-ray diffraction, scanning electron microscopy, and

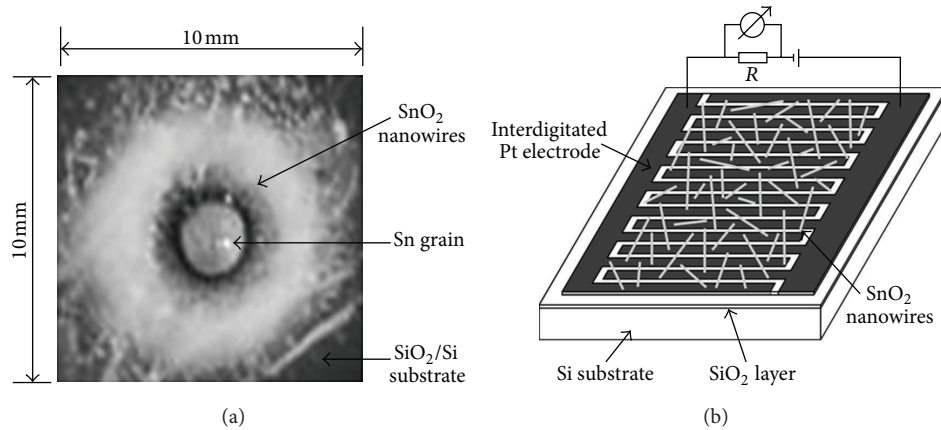


FIGURE 1: (a) Photograph of the obtained SnO_2 nanowires. (b) Schematic illustration of SnO_2 nanowire gas sensor device.

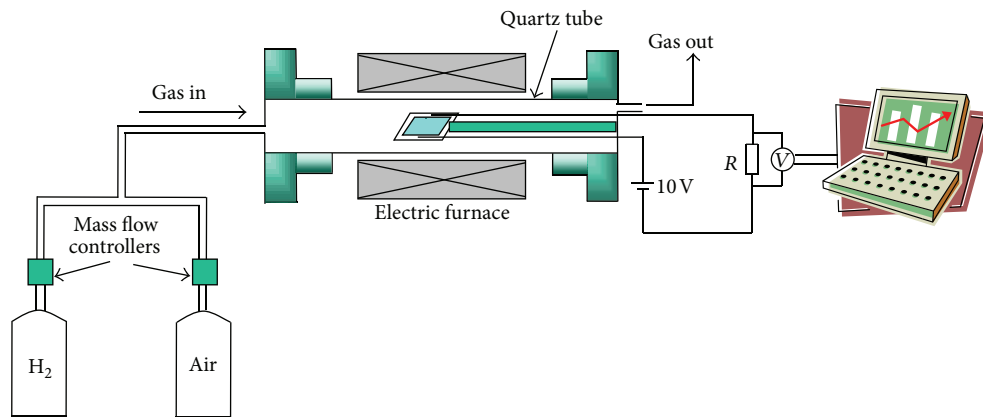


FIGURE 2: Apparatus used for the measurement of H_2 gas sensing properties.

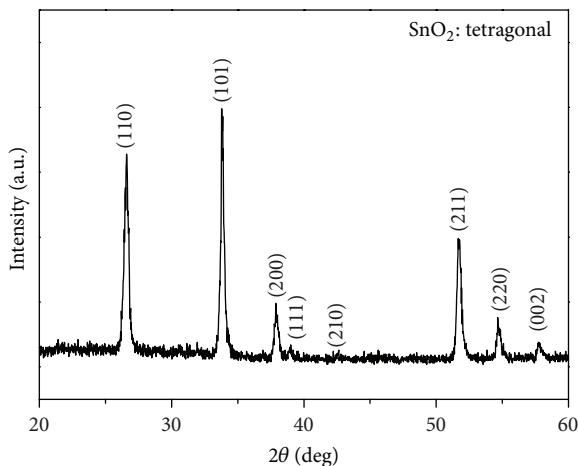


FIGURE 3: XRD pattern of SnO_2 nanowires.

transmission electron microscopy. The Fourier transform infrared spectrum and growth mechanism of the nanowires were also investigated and discussed. The measurements of H_2 gas sensing properties demonstrated that SnO_2 nanowire gas sensor obtained peak sensitivity at a low operating

temperature of 150°C and showed reversible response to H_2 gas (100–1000 ppm) at an operating temperature of $\text{RT}-300^\circ\text{C}$.

2. Experimental

SnO_2 nanowires were synthesized on oxidized Si substrates by thermal evaporation of tin grains. Tin grains with high purity of 99.9% were placed on oxidized Si substrates in an alumina boat. No catalysts or impurities were introduced. The alumina boat was introduced at the center of a quartz tube that was inserted in a horizontal tube furnace. Ar gas with a flow rate of 50 mL min^{-1} was introduced into the quartz tube at ambient pressure. Then, the furnace was heated to 900°C and maintained at this temperature for 1 h. After the furnace was cooled down to room temperature naturally, a layer of wire-shaped products was obtained on the substrates around the tin grains, as shown in Figure 1(a).

The crystallographic structure of SnO_2 nanowires was studied by means of glancing angle X-ray diffractometer (GAXRD) (Shimadzu XRD-6100) with $\text{Cu K}\alpha$ radiation. The morphology was observed by field emission scanning electron microscope (FESEM) (JEOL JSM-6700F). The microstructure and components were investigated by transmission electron microscope (TEM) (JEOL EM002B)

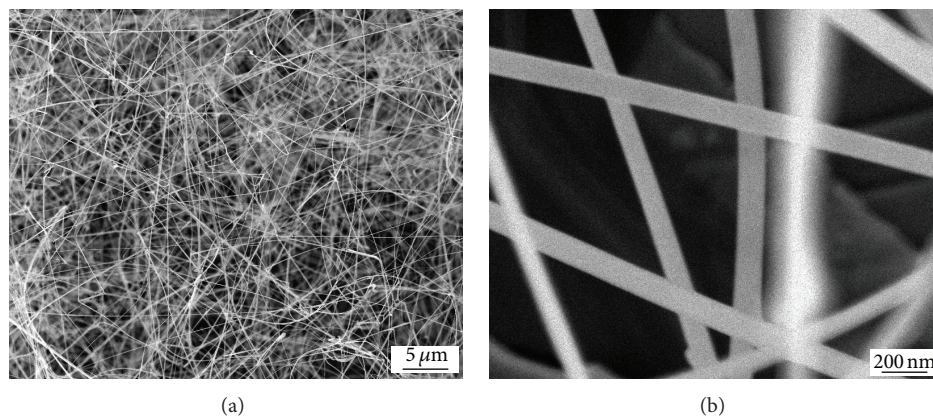


FIGURE 4: (a) Low magnification and (b) high magnification FESEM images of SnO₂ nanowires.

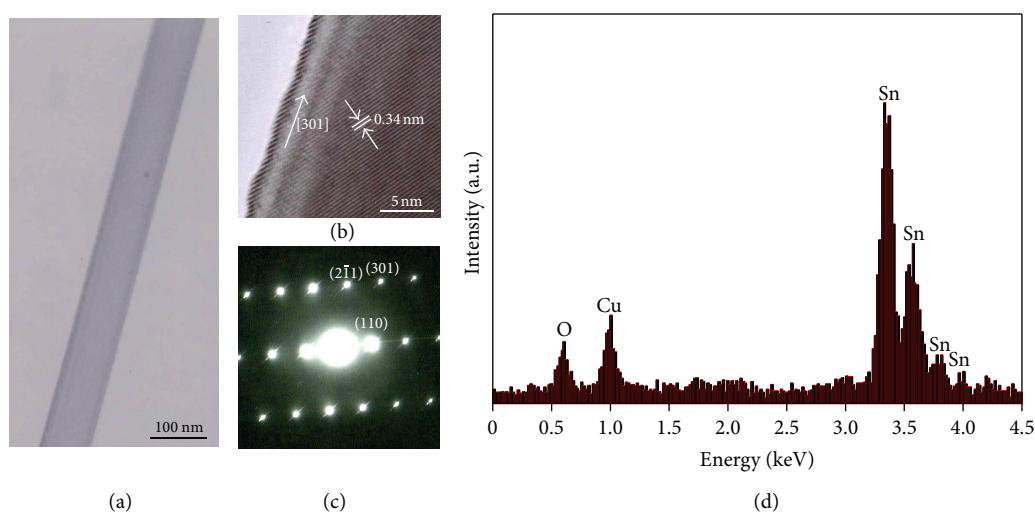


FIGURE 5: (a) TEM image of a single SnO₂ nanowire with a diameter of 96 nm. (b) HRTEM image of this nanowire. (c) SAED pattern of this nanowire. (d) EDX analysis of this nanowire.

with an energy dispersive X-ray spectrometer (EDX). The Fourier transform infrared (FTIR) spectrum was measured by infrared spectrometer (Shimadzu IRPrestige-21).

SnO₂ nanowire gas sensor was fabricated by pouring a few drops of nanowire-suspended ethanol onto oxidized Si substrate with a pair of interdigitated Pt electrodes. The schematic illustration of a SnO₂ nanowire gas sensor device is shown in Figure 1(b). H₂ gas sensing properties were measured in a quartz tube inserted in an electric furnace at the operating temperatures ranging from room temperature (RT ≈ 25°C) to 300°C. As shown in Figure 2, dry synthetic air mixed with the desired concentration of H₂ gas flowed through the quartz tube at a rate of 200 mL min⁻¹. The electrical measurement was carried out by a volt-amperometric method at a constant bias of 10 V, and a multimeter (Agilent 34970A) was used to monitor the change of electrical resistance upon turning H₂ gas on and off. In this study, the sensor sensitivity was defined as $S = (R_a - R_g)/R_g$, where R_a and R_g were the electrical resistances before and after the introduction of H₂ gas, respectively.

3. Results and Discussion

3.1. Structure and Morphology. The XRD pattern of the obtained SnO₂ nanowires is shown in Figure 3. All the diffraction peaks can be indexed to the tetragonal SnO₂ structure with lattice constants of $a = b = 0.4738$ nm and $c = 0.3187$ nm according to JCPDS card no. 41-1445. Moreover, no other crystalline forms such as Sn or SnO are detected, indicating that single phase SnO₂ nanowires are obtained.

Figure 4(a) is a typical FESEM image of SnO₂ nanowires, showing that a large quantity of wire-shaped nanostructures can be produced. It is found that SnO₂ nanowires have diameters ranging from 30 to 200 nm and have lengths of several tens of micrometers. A high magnification FESEM image shown in Figure 4(b) indicates that SnO₂ nanowires have smooth sidewalls.

Figure 5(a) is a typical TEM image of a single SnO₂ nanowire with a diameter of 96 nm. A high-resolution TEM (HRTEM) image of this nanowire is shown in Figure 5(b), in which the lattice planes can be clearly seen, indicating a

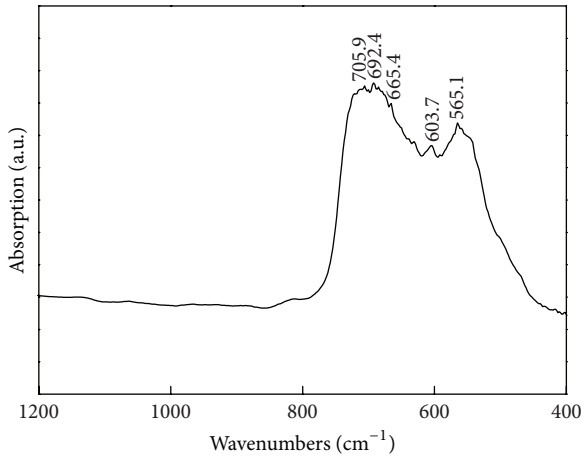


FIGURE 6: FTIR spectrum of SnO₂ nanowires.

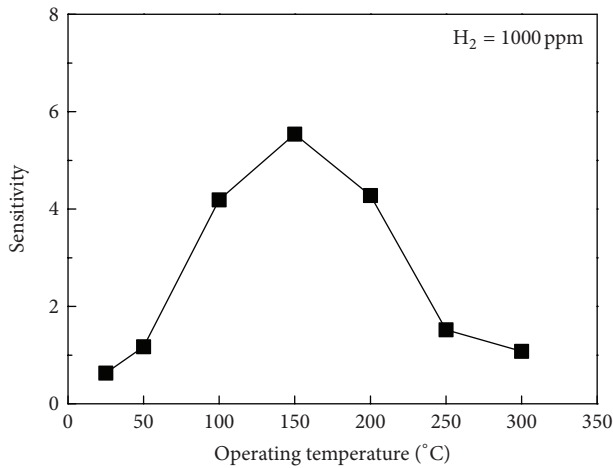


FIGURE 7: The sensitivity of SnO₂ nanowire gas sensor as a function of the operating temperature upon exposure to 1000 ppm H₂ gas.

single crystal structure. The interplanar spacing of 0.34 nm corresponds to the (110) plane in a tetragonal SnO₂ structure. The corresponding selected area electron diffraction (SAED) pattern shown in Figure 5(c) also supports the formation of single crystal tetragonal SnO₂ nanowires. The growth direction of SnO₂ nanowires is found to be [301], which is consistent with previous reports [24, 25]. To demonstrate the chemical composition of the nanowire, EDX analysis was performed, and the EDX spectrum is illustrated in Figure 5(d). We can see that, except for the Cu element from the copper grid, only peaks of Sn and O elements are observed.

3.2. The Growth Mechanism. Two models have been proposed to describe the growth mechanism of SnO₂ nanowires: the catalyst-assisted vapour-liquid solid (VLS) and the vapour-solid (VS) growth mechanisms [2]. The VLS mechanism was first proposed by Wagner and Ellis in 1964 [26]. The important feature of the VLS growth process is the existence of metal nanoparticles. The nanoparticles serve as

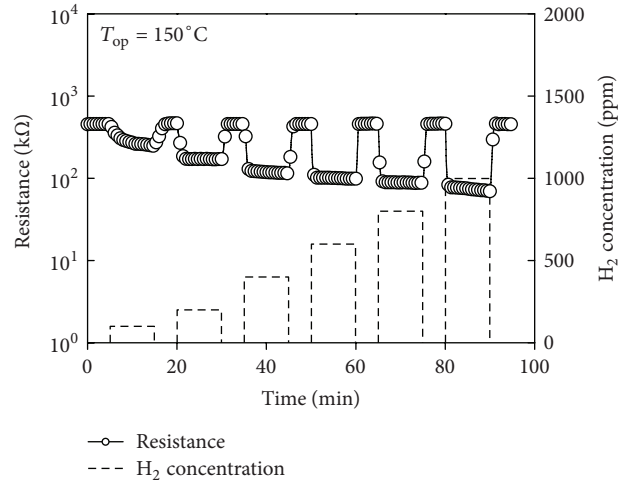


FIGURE 8: Dynamic response of SnO₂ nanowire gas sensor to H₂ gas with various concentrations at 150°C.

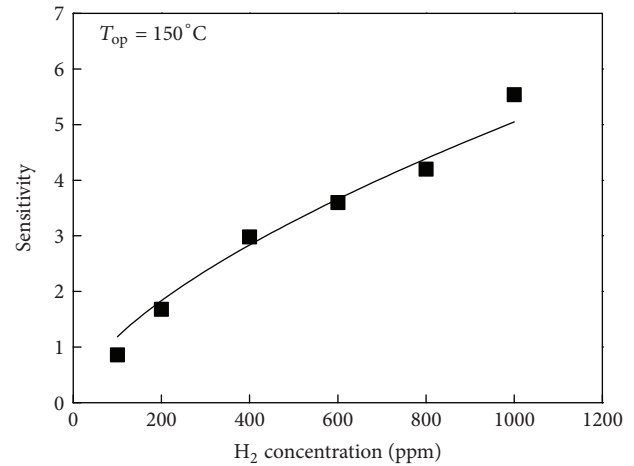


FIGURE 9: The relationship between the sensor sensitivity and H₂ concentration at the operating temperature of 150°C.

catalysts between the vapour feed and the solid product and usually locate at the ends of the produced nanowires [27]. In this study, no metal catalysts were employed, and no metal nanoparticles were observed at any ends of SnO₂ nanowires. Therefore, the growth process might be dominated by the VS growth mechanism. At a high temperature of 900°C, tin grains are vaporized and then directly condensed on the substrates. Once the condensation process happens, the initial condensed molecules form seed crystals serving as the nucleation sites. As a result, they facilitate directional growth to minimize the surface energy [2]. Therefore, SnO₂ nanowires tend to be produced by continuous aggregation of more molecular SnO₂ on the growth front of the initial SnO₂ nuclei via the VS growth mechanism [28].

3.3. FTIR Spectrum. The FTIR spectrum of SnO₂ nanowires is shown in Figure 6. Compared with the data published in the literatures [29–31], the peaks observed can be determined.

The peaks located at 603.7 and 692.4 cm^{-1} can be attributed to the Sn–O stretching vibration in SnO_2 . The peaks at 665.4 and 705.9 cm^{-1} can be assigned to O–Sn–O bending vibration. The peak at 565.1 cm^{-1} is noticeable because it cannot be found in the FTIR spectrum of bulk SnO_2 and is similar to the surface vibration mode of the peak at 564 cm^{-1} in SnO_2 nanopowders resulting from the nanosize effect [32]. This surface vibration mode is related to the change of the surface structure. When the influence of the volume atoms on the lattice energy of surface atoms decreases, the surface tensile stress decreases, leading to the renormalization of the surface atoms and forming the new vibration mode [31, 32].

3.4. H_2 Gas Sensing Properties. SnO_2 nanowires are very promising due to their large surface-to-volume ratio and great surface activity, which make them ideal candidates for gas sensing materials. Figure 7 shows the sensitivity of SnO_2 nanowire gas sensor as a function of the operating temperature upon exposure to 1000 ppm H_2 gas. It is found that the sensitivity increases with increasing operating temperature below 150°C, but reverse tendency is observed after 150°C. At this optimum temperature of 150°C, the highest sensitivity of 5.54 is obtained. It should be noted that the value of this peak sensitivity is larger than that of a porous SnO_2 sputtered thin film deposited at 24 Pa and RT upon exposure to 1000 ppm H_2 gas [33]. In addition, the sensitivity value is comparable to the one found in [22] and is even higher than the value reported in [21, 23] for SnO_2 nanowires, showing that the obtained SnO_2 nanowires are good for gas sensing application.

Figure 8 shows the dynamic responses of SnO_2 nanowire gas sensor to H_2 gas with various concentrations at 150°C. One can see that the resistance decreases upon exposure to H_2 gas and the resistance further decreases with increasing H_2 concentration. In addition, the resistance can recover to its initial value after removing H_2 gas, indicating a good reversibility of SnO_2 nanowire gas sensor. The resistance changes of 0.86, 1.68, 2.98, 3.61, 4.19, and 5.54 times with respect to the baseline are observed towards 100, 200, 400, 600, 800, and 1000 ppm H_2 gas, respectively. The sensor also shows reversible response to H_2 gas with different concentrations at an operating temperature of RT–300°C, although the corresponding data are not shown in this figure.

The relationship between the sensor sensitivity and H_2 concentration at the operating temperature of 150°C is shown in Figure 9. It is found that the sensitivity increases as H_2 concentration increases. Such a variation implies that the sensitivity S can be described as a function of gas concentration C by an empirical model of $S = aC^b$, where a and b are constants for a given gas. In this study, “ a ” and “ b ” were found to be 0.065 ± 0.034 and 0.629 ± 0.079 , respectively. We see that the experimental data and the theoretical curve obtained from the empirical model show good agreement.

4. Conclusions

Single-crystalline SnO_2 nanowires were synthesized on oxidized silicon substrates by thermal evaporation of tin grains at 900°C. The structural characteristics, growth mechanism,

and H_2 gas sensing properties of SnO_2 nanowires were investigated. SnO_2 nanowires with a tetragonal structure are 30–200 nm in diameter and several tens of micrometers in length. The nanosize effect induced FTIR surface vibration mode with peak at 565.1 cm^{-1} was observed. The formation of SnO_2 nanowires follows a vapour-solid (VS) growth mechanism. SnO_2 nanowire gas sensor shows reversible response to H_2 gas at an operating temperature of RT–300°C. The peak sensitivity is found at a low operating temperature of 150°C. The sensor sensitivity increases empirically with an increase of H_2 gas concentration. The results demonstrate the potential of SnO_2 nanowires for gas sensor applications.

Acknowledgments

The authors acknowledge the supports to the project given by the Fundamental Research Funds for the Central Universities (Grant no. N120501002), Program for Liaoning Excellent Talents in University (Grant no. LJQ2013025), and National Science and Technology Major Project of the Ministry of Science and Technology of China (Grant no. 2012ZX07202003).

References

- [1] A. Vaseashta and D. Dimova-Malinovska, “Nanostructured and nanoscale devices, sensors and detectors,” *Science and Technology of Advanced Materials*, vol. 6, no. 3-4, pp. 312–318, 2005.
- [2] J. G. Lu, P. C. Chang, and Z. Y. Fan, “Quasi-one-dimensional metal oxide materials—synthesis, properties and applications,” *Materials Science and Engineering R*, vol. 52, no. 1–3, pp. 49–91, 2006.
- [3] Y. P. Yadava, G. Denicoló, A. C. Arias, L. S. Roman, and I. A. Hümmelgen, “Preparation and characterization of transparent conducting tin oxide thin film electrodes by chemical vapour deposition from reactive thermal evaporation of SnCl_2 ,” *Materials Chemistry and Physics*, vol. 48, no. 3, pp. 263–267, 1997.
- [4] D. Vaufrey, M. Ben Khalifa, M. P. Besland et al., “Reactive ion etching of sol-gel-processed SnO_2 transparent conducting oxide as a new material for organic light emitting diodes,” *Synthetic Metals*, vol. 127, no. 1–3, pp. 207–211, 2002.
- [5] T. Yamazaki, H. Okumura, C.-J. Jin, A. Nakayama, T. Kikuta, and N. Nakatani, “Effect of density and thickness on H_2 -gas sensing property of sputtered SnO_2 films,” *Vacuum*, vol. 77, no. 3, pp. 237–243, 2005.
- [6] Y. Shimizu, A. Jono, T. Hyodo, and M. Egashira, “Preparation of large mesoporous SnO_2 powder for gas sensor application,” *Sensors and Actuators B*, vol. 108, no. 1-2, pp. 56–61, 2005.
- [7] J. C. Chou and Y. F. Wang, “Preparation and study on the drift and hysteresis properties of the tin oxide gate ISFET by the sol-gel method,” *Sensors and Actuators B*, vol. 86, no. 1, pp. 58–62, 2002.
- [8] W.-P. Tai and K. Inoue, “Eosin Y-sensitized nanostructured $\text{SnO}_2/\text{TiO}_2$ solar cells,” *Materials Letters*, vol. 57, no. 9-10, pp. 1508–1513, 2003.
- [9] J.-S. Lee, S.-K. Sim, B. Min, K. Cho, S. W. Kim, and S. Kim, “Structural and optoelectronic properties of SnO_2 nanowires synthesized from ball-milled SnO_2 powders,” *Journal of Crystal Growth*, vol. 267, no. 1-2, pp. 145–149, 2004.

- [10] Z. Ying, Q. Wan, Z. T. Song, and S. L. Feng, "Controlled synthesis of branched SnO₂ nanowhiskers," *Materials Letters*, vol. 59, no. 13, pp. 1670–1672, 2005.
- [11] X. Y. Xue, Y. J. Chen, Y. G. Liu, S. L. Shi, Y. G. Wang, and T. H. Wang, "Synthesis and ethanol sensing properties of indium-doped tin oxide nanowires," *Applied Physics Letters*, vol. 88, no. 20, Article ID 201907, 2006.
- [12] D. Calestani, M. Zha, G. Salviati et al., "Nucleation and growth of SnO₂ nanowires," *Journal of Crystal Growth*, vol. 275, no. 1-2, pp. e2083–e2087, 2005.
- [13] W. Zhu, W. Z. Wang, H. L. Xu, and J. L. Shi, "Fabrication of ordered SnO₂ nanotube arrays via a template route," *Materials Chemistry and Physics*, vol. 99, no. 1, pp. 127–130, 2006.
- [14] G. Cheng, K. Wu, P. Zhao, Y. Cheng, X. L. He, and K. X. Huang, "Solvochemical controlled growth of Zn-doped SnO₂ branched nanorod clusters," *Journal of Crystal Growth*, vol. 309, no. 1, pp. 53–59, 2007.
- [15] E. Comini, G. Faglia, G. Sberveglieri, D. Calestani, L. Zanotti, and M. Zha, "Tin oxide nanobelts electrical and sensing properties," *Sensors and Actuators B*, vol. 111-112, pp. 2–6, 2005.
- [16] E. Comini, G. Faglia, G. Sberveglieri, Z. Pan, and Z. L. Wang, "Stable and highly sensitive gas sensors based on semiconducting oxide nanobelts," *Applied Physics Letters*, vol. 81, no. 10, pp. 1869–1871, 2002.
- [17] A. Kolmakov, Y. X. Zhang, G. S. Cheng, and M. Moskovits, "Detection of CO and O₂ using tin oxide nanowire sensors," *Advanced Materials*, vol. 15, no. 12, pp. 997–1000, 2003.
- [18] H. Huang, O. K. Tan, Y. C. Lee, T. D. Tran, M. S. Tse, and X. Yao, "Semiconductor gas sensor based on tin oxide nanorods prepared by plasma-enhanced chemical vapor deposition with postplasma treatment," *Applied Physics Letters*, vol. 87, no. 16, Article ID 163123, 2005.
- [19] N. S. Ramgir, I. S. Mulla, and K. P. Vijayamohanan, "A room temperature nitric oxide sensor actualized from Ru-doped SnO₂ nanowires," *Sensors and Actuators B*, vol. 107, no. 2, pp. 708–715, 2005.
- [20] D.-F. Zhang, L.-D. Sun, G. Xu, and C.-H. Yan, "Size-controllable one-dimensional SnO₂ nanocrystals: synthesis, growth mechanism, and gas sensing property," *Physical Chemistry Chemical Physics*, vol. 8, no. 42, pp. 4874–4880, 2006.
- [21] S. Deshpande, A. Karakoti, G. Londe, H. J. Cho, and S. Seal, "Room temperature hydrogen detection using 1-D nanostructured tin oxide sensor," *Journal of Nanoscience and Nanotechnology*, vol. 7, no. 9, pp. 3354–3357, 2007.
- [22] Y. L. Wang, X. C. Jiang, and Y. N. Xia, "A solution-phase, precursor route to polycrystalline SnO₂ nanowires that can be used for gas sensing under ambient conditions," *Journal of the American Chemical Society*, vol. 125, no. 52, pp. 16176–16177, 2003.
- [23] A. Kolmakov, D. O. Klenov, Y. Lilach, S. Stemmer, and M. Moskovits, "Enhanced gas sensing by individual SnO₂ nanowires and nanobelts functionalized with Pd catalyst particles," *Nano Letters*, vol. 5, no. 4, pp. 667–673, 2005.
- [24] J. X. Wang, D. F. Liu, X. Q. Yan et al., "Growth of SnO₂ nanowires with uniform branched structures," *Solid State Communications*, vol. 130, no. 1-2, pp. 89–94, 2004.
- [25] Y. Chen, X. Cui, K. Zhang et al., "Bulk-quantity synthesis and self-catalytic VLS growth of SnO₂ nanowires by lower-temperature evaporation," *Chemical Physics Letters*, vol. 369, no. 1-2, pp. 16–20, 2003.
- [26] R. S. Wagner and W. C. Ellis, "Vapor-liquid-solid mechanism of single crystal growth," *Applied Physics Letters*, vol. 4, no. 5, pp. 89–90, 1964.
- [27] E. Comini, "Metal oxide nano-crystals for gas sensing," *Analytica Chimica Acta*, vol. 568, no. 1-2, pp. 28–40, 2006.
- [28] T. Gao and T. Wang, "Vapor phase growth and optical properties of single-crystalline SnO₂ nanobelts," *Materials Research Bulletin*, vol. 43, no. 4, pp. 836–842, 2008.
- [29] Z. Huang and C. Chai, "Water-assisted growth and characterization of SnO₂ nanobelts," *Materials Letters*, vol. 61, no. 29, pp. 5113–5116, 2007.
- [30] D. Amalric-Popescu and F. Bozon-Verduraz, "Infrared studies on SnO₂ and Pd/SnO₂," *Catalysis Today*, vol. 70, no. 1-3, pp. 139–154, 2001.
- [31] L. J. Li, F. J. Zong, X. D. Cui et al., "Structure and field emission properties of SnO₂ nanowires," *Materials Letters*, vol. 61, no. 19-20, pp. 4152–4155, 2007.
- [32] L. Abello, B. Bochu, A. Gaskov, S. Koudryavtseva, G. Lucazeau, and M. Roumyantseva, "Structural characterization of nanocrystalline SnO₂ by X-ray and Raman spectroscopy," *Journal of Solid State Chemistry*, vol. 135, no. 1, pp. 78–85, 1998.
- [33] Y. B. Shen, T. Yamazaki, Z. F. Liu, C. J. Jin, T. Kikuta, and N. Nakatani, "Porous SnO₂ sputtered films with high H₂ sensitivity at low operation temperature," *Thin Solid Films*, vol. 516, no. 15, pp. 5111–5117, 2008.



Hindawi

Submit your manuscripts at
<http://www.hindawi.com>

